Sensors and Materials, Vol. 33, No. 8 (2021) 2719–2733
MYU Tokyo

S & M 2651

Development of Improved pH Module and Miniaturized Water Quality Detection System

Hsing-Cheng Yu,[1*] Chung-Kai Chi,[1] Ming-Yang Tsai,[1]
Chun-Lin Cheng,[1] Jung-How Wang,[2] and Szu-Ju Li[2]

[1]Department of Systems Engineering and Naval Architecture, National Taiwan Ocean University,
2 Pei-Ning Road, Keelung 20224, Taiwan
[2]Material and Chemical Research Laboratories, Industrial Technology Research Institute,
195, Sec. 4, Chung Hsing Road, Chutung, Hsinchu 31040, Taiwan

(Received April 17, 2020; accepted May 13, 2021)

Keywords: fluorine-doped tin oxide (FTO), pH module, water quality detection

In recent years, many cases of water pollution have been caused by industrial wastewater. Industrial wastewater containing heavy metal pollution is discharged into the groundwater, causing land and environmental pollution and affecting human health. Hence, the development of a miniaturized water quality detection system (WQDS) to protect water resources is of great urgency. A miniaturized WQDS has the advantages of multiple parameter detection, continuous monitoring, miniaturized dimensions, high sensitivity, and accuracy. The representative water quality parameters monitored by the WQDS were temperature, pH, electrical conductivity, and copper ion (Cu^{2+}) concentration. In addition, fluorine-doped tin oxide (FTO) was substituted for indium tin oxide (ITO) in this study to fabricate an improved pH-sensing module that reduces the interaction between subsystems, improves the measurement accuracy, enhances convenience, and reduces the manufacturing cost of the sensor chips. Electrodes combined with FTO conductive glass were designed and fabricated to achieve the miniaturized WQDS as a system on a chip. The miniaturized WQDS exhibits good potential for the precise detection of various water quality parameters and for application in the water-monitoring field.

1. Introduction

In the last few decades, industrial wastewater containing heavy metals has been continuously polluting Taiwan, causing water and environmental pollution. Industrial waste that is discharged before being purified might affect human health and the environment. Thus, the development of a water quality detection system (WQDS) using advanced sensing technology, signal processing, big data analysis, and cloud database technology is very important.(1) A fixed water quality monitoring system with wireless communication was developed in our previous study.(2) In order to detect the degree of water pollution, partial-functional water quality indicators have been adopted to analyze the physical (e.g., temperature, odor, turbidity, electrical conductivity) and chemical (e.g., pH, copper ion concentration, chemical oxygen content) properties of water. The temperature of water indirectly affects its electrical conductivity, dissolved oxygen, and

*Corresponding author: e-mail: hcyu@ntou.edu.tw
https://doi.org/10.18494/SAM.2021.3352

ISSN 0914-4935

other properties. The pH value is the concentration of hydrogen ions in water. Aquatic organisms are highly sensitive to the pH of water, and an appropriate pH is very important for their survival. An indium tin oxide (ITO) film was electrodeposited as a sensing material to fabricate a pH-sensing electrode in a previous study.(2) A fluorine-doped tin oxide (FTO) film has been substituted for an ITO film to fabricate an improved pH-sensing electrode to reduce the interaction between subsystems, improve measurement accuracy, enhance convenience, and reduce the cost of manufacturing sensor chips. Consequently, in this study, we present the design and manufacture of electrodes combined with FTO conductive glass to achieve a miniaturized WQDS as a system on a chip. Moreover, the electrical conductivity, which is related to the ionic strength of water, can be used to infer the mass of dissolved substances in water.(3) It can also be utilized to determine whether water is contaminated or the degree of saltwater injection in coastal areas. The copper ion concentration in ordinary water is between 20 and 75 ppb.(4) However, there may be a high concentration of copper ions in wastewater that has passed through old metal pipes or electroplating plants, causing human health problems and environmental pollution. Thus, a series of standard policies have been formulated by the US Environmental Protection Agency to limit the concentration of copper ions. The maximum allowable concentration in lakes and rivers is 1 ppm, and the concentration of copper ions in drinking water must be less than 1.3 ppm.(5) Water quality parameters have been provided by the environmental water quality monitoring information network of the Environmental Protection Administration under Executive Yuan of Republic of China (Taiwan). The pollutant content of industrial wastewater is measured directly to obtain chemical, physical, and biological data, which are compared with the wastewater pollutant limits in water quality standards(6) to assess whether the water quality is acceptable. Additionally, industrial wastewater has to satisfy the regulations of the national environmental water quality monitoring information network of the Environmental Protection Administration under Executive Yuan of Republic of China (Taiwan). For example, the temperature must be below 38 °C, the pH should be from 6.0 to 9.0, and the copper ion content should be 3.0 ppm or lower.(7) To help satisfy these regulations, it is desirable to develop a miniaturized WQDS with multiple functions, a low cost, and high durability to simultaneously detect multiple water quality parameters such as temperature, pH, electrical conductivity, and copper ion concentration.

2. Measurement Principle and System Design

This study presents a multifunctional miniaturized WQDS for continuous monitoring, which can simultaneously measure the water parameters of temperature, pH, electrical conductivity, and copper ion concentration. Figure 1 shows a block diagram of the miniaturized WQDS. It consists of four circuit modules: a wireless transmitter module, cleaning module, pH-EC-temperature module, and copper ion measurement module.

2.1 Measurement of temperature

The circuit for measuring the temperature in the pH-EC-temperature module is shown in Fig. 2. Typically, the temperature is measured indirectly by measuring the change in resistance with

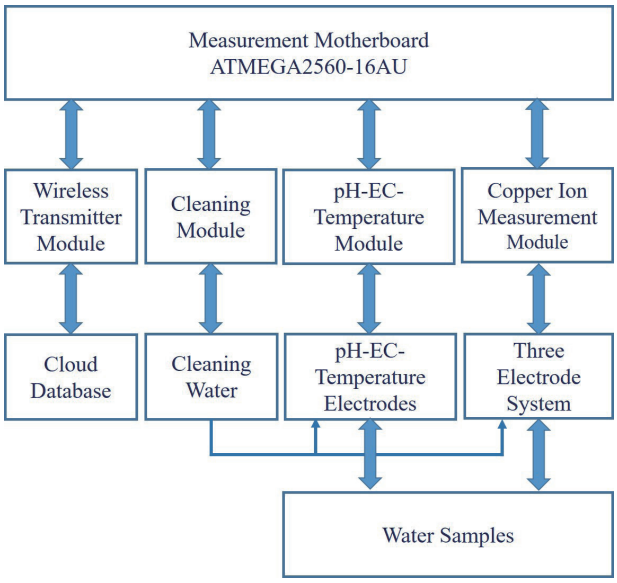

Fig. 1. (Color online) Block diagram of the miniaturized WQDS system.

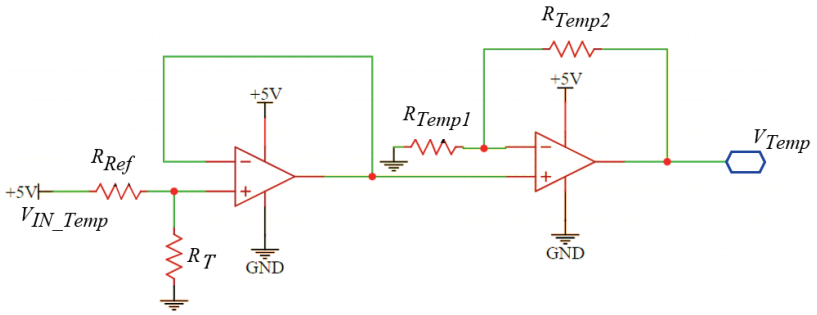

Fig. 2. (Color online) Circuit for measuring the temperature in the pH-EC-temperature module.

the temperature using a negative temperature coefficient (NTC) thermistor and the relationship between temperature and resistance in Eq. (1), where R_T is the measurement resistance at temperature T and R_{Ref} is a reference resistance. First, it can be observed that the voltage V_{IN_Temp} is 5 V in a general voltage divider circuit. Following the voltage divider circuit design of the NTC thermistor, i.e., two series resistors R_T and R_{Ref}, the signal enters a buffer amplifier circuit, then passes into a second-stage non-inverting amplifier to adjust the magnification, and then enters a microcontroller unit (MCU). The thermal voltage V_{Temp} related to the temperature characteristics is captured by an analog-to-digital converter (ADC) in the temperature measurement circuit. V_{Temp} can be expressed as

$$V_{Temp} = \frac{R_T}{R_{Ref}} \cdot \left(1 + \frac{R_{Temp2}}{R_{Temp1}}\right) \cdot V_{IN\_Temp}, \tag{1}$$

where R_T is the resistance of the NTC thermistor, R_{Ref} is the reference resistance, and R_{Temp1} and R_{Temp2} are the input resistance and feedback resistance of the non-inverting amplifier in the temperature measurement circuit, respectively. Furthermore, the closed-loop gain can be adjusted via the values of R_{Temp1} and R_{Temp2} in the non-inverting amplifier in the temperature measurement circuit.

2.2 Measurement of pH value

To improve the shortcomings of ion-sensitive field-effect transistors, van der Spiegel *et al.* proposed a new structure for an extended-gate field-effect transistor (EGFET). The structure includes a metal-oxide-semiconductor field-effect transistor, which retains a metal gate electrode and uses a signal wire to connect the separated low-impedance conductive films and the field-effect transistor.[8] This allows EGFET devices to solve the problem of fragility. The principle of adsorption bonding was proposed by Yates.[9] Hydrogen ions bond with a conductive film in an aqueous solution, and the hydrogen ions are adsorbed on the surface of the conductive film, changing the surface potential and enabling the measurement of the pH value.[10] The adoption of FTO has the advantage of good chemical (acid and alkali) resistance, and the ITO conductive film exhibits strong water absorption.[11] The material must be protected from moisture to avoid contamination with hydroxide ions and carbon dioxide, which could easily cause chemical reactions with the material and deteriorate the ITO.[12,13] The surface layer is composed of tiny crystals. During the measurement process, the temperature rise reduces the crystal surface fission and reduces the crystal interface. At this time, in order to free electrons, it consumes a relatively large amount of energy. Therefore, the temperature rise exceeds 3 °C during the measurement. The resistance of a conductive film is proportional to the temperature.[14] The FTO film substrate is a 0.5-mm-thick transparent soda lime glass plate, which is coated with 180–200-nm-thick FTO by spray pyrolysis. Specifically, the resistivity of the FTO conductive glass film is 9–11 Ω/cm^2 and the transmittance is 550 nm. We cut a sample of 10 mm width and 10 mm length, washed it with soapy water, and then rinsed it with deionized water, which was followed by ultrasonic treatment in acetone to remove impurities.

The circuit for measuring the pH value in the pH-EC-temperature module is shown in Fig. 3. The FTO conductive film from the improved pH-sensing electrode is used as a working

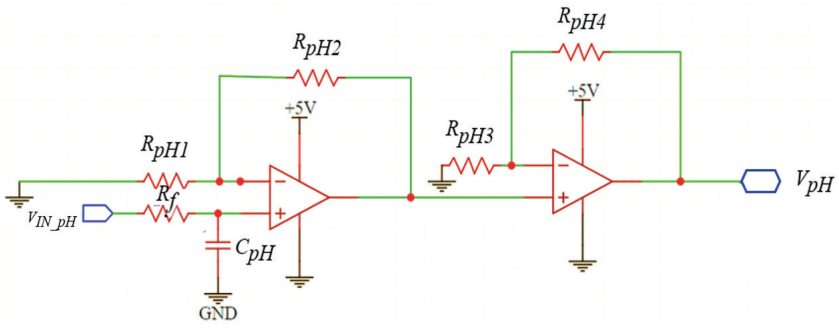

Fig. 3. (Color online) Circuit for measuring the pH value in the pH-EC-temperature module.

electrode, and a Ag/AgCl reference electrode is connected to provide the electrode with a stable electric potential. Its electric potential is not affected by changes in the composition of the solution to be measured. The voltage V_{IN_pH} is the input electric potential signal, which is obtained by the FTO conductive film of the working electrode, and passes through an active low-pass filter, which is constructed using a resistor R_f and capacitor C_{ph} network, to avoid unnecessary high-frequency noise. The input electric potential signal circulates the input terminal of a first-stage non-inverting amplifier, and then connects with the second-stage non-inverting amplifier. The discrete pH value is set between pH 4.0 and 10.0. The acid-base voltage, i.e., V_{pH}, acquired by the ADC in the pH measurement circuit is given by

$$V_{pH} = \left(1 + \frac{R_{pH2}}{R_{pH1}}\right)\left(1 + \frac{R_{pH4}}{R_{pH3}}\right) \cdot V_{IN\_pH}\,, \tag{2}$$

where the closed-loop gain of the first-stage non-inverting amplifier can be adjusted via the values of the input resistance R_{pH1} and the feedback resistance R_{pH2} in the pH measurement circuit, and the closed-loop gain of the second-stage non-inverting amplifier can be adjusted via the values of the input resistance R_{pH3} and the feedback resistance R_{pH4} in the pH measurement circuit.

2.3 Measurement of electrical conductivity

The product of the electrical conductivity and electric field strength E is equal to the conducted current strength J. The SI unit of the electrical conductivity is Siemens per meter (S/m), and S is the reciprocal of resistance. The speed of ions is affected by temperature; the higher the temperature, the faster the ion movement. Electrical conductivity measurement is a typical way of measuring the ionic content (anions and cations) in a solution, where the higher the temperature, the greater the electrical conductivity; in general, the electrical conductivity increases by 1.9% for every 1 °C increase.[15] Electrical conductivity represents the difficulty of ion flow in a solution, and the electrical conductivity is proportional to the current. Under the measurement experiments, bipolar electrodes (two parallel plate electrodes) are used to measure the electrical conductivity by applying an alternating current. The bipolar electrodes are inserted into the test solution to measure the voltage, and then the resistance of the test solution is estimated. The reciprocal of the resistance is the electrical conductivity.

The circuit for measuring the electrical conductivity in the pH-EC-temperature module is shown in Fig. 4. When the bipolar electrodes of the electrical conductivity sensor are inserted into the test solution, the resistance R_{EC} changes with the position of the dual gold-plated electrodes, and the voltage V_{IN_EC} is the AC signal flowing through the input of the non-inverting amplifier. The AC signal is generated by a single-supply 5 V Wein bridge oscillator circuit, and the amplifier output is connected to a resistor via a half-wave rectifier circuit to avoid the diode off. The terminal voltage of the reverse input signal is floating, and the circuit characteristics are similar to those of an ideal diode. A capacitor C_{EC} is connected to avoid the

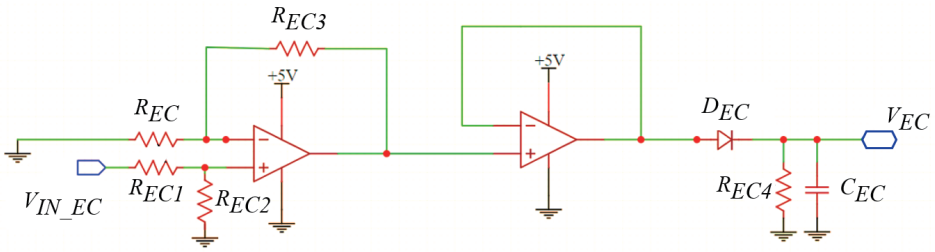

Fig. 4. (Color online) Circuit for measuring the electrical conductivity in the pH-EC-temperature module.

generation of ripple waves. The voltage for measuring the electrical conductivity, i.e., V_{EC}, captured by the ADC in the measurement circuit of the electrical conductivity is given by

$$V_{EC} = \left(\frac{R_{EC2}}{R_{EC1} + R_{EC2}} \right) \cdot \left(1 + \frac{R_{EC3}}{R_{EC}} \right) \cdot V_{IN\_EC}, \tag{3}$$

where R_{EC} and R_{EC1} are the input resistances, R_{EC2} is the grounded resistance, and R_{EC3} is the feedback resistance of the non-inverting amplifier in the measurement circuit of the electrical conductivity. Hence, the closed-loop gain can be adjusted using the resistance values R_{EC} and R_{EC3} in the non-inverting amplifier of the circuit used to measure the electrical conductivity.

2.4 Measurement of copper ion concentration

Copper is an important trace element for sustaining human life, but too much or too little ingestion of copper can cause conditions of copper excess or deficiency in the human body. When the copper ion concentration in water reaches 0.01 ppm, the self-purification ability of the water is inhibited. When the copper ion concentration in water exceeds 3.0 ppm, the water has a distinct smell.[16] In this study, the three electrodes of the copper ion concentration sensor are a gold-plated working electrode, a silver/silver chloride (Ag/AgCl) reference electrode, and a platinum auxiliary electrode. A large number of electrons are transferred in oxidation-reduction and applied on the gold-plated working electrode to measure the electric potential and determine the metal ion concentration in the solution. Square wave voltammetry (SWV) was utilized to detect the heavy metal ion concentration in water.[17] In the SWV, the potential–current curve is derived from the pulse amplitude, which varies according to the fixed electric potential step and period.[18,19] The SWV offers good sensitivity and high resistance to capacitive currents. All characteristic currents in the potential–current curve can be measured at the end of each half period, including the variations in the height and width of the potential pulse, so the currents are measured at the end of the forward and reverse pulses. Hence, the electric potential signal can be converted to the characteristic current in the potential–current curve. The difference in the characteristic current can be converted to the copper ion concentration.[20,21]

The circuit in the module for measuring the copper ion concentration is shown in Fig. 5. The output voltage used to measure the copper ion concentration, i.e., V_{Cu}, is given by

$$V_{\mathrm{Cu}} = \left(\frac{R_{\mathrm{Cu2}}}{R_{\mathrm{Cu1}} + R_{\mathrm{Cu2}}} \right) \cdot \left(1 + \frac{R_{\mathrm{Cu3}}}{R_{\mathrm{Cu}}} \right) \cdot V_{IN\_\mathrm{Cu}}, \tag{4}$$

where V_{IN_Cu} is the measurement voltage signal of the gold-plated working electrode, R_{Cu} and R_{Cu1} are the input resistances, R_{Cu2} is the grounded resistance, and R_{Cu3} is the feedback resistance of the non-inverting amplifier in the measurement circuit of the copper ion concentration. Furthermore, the closed-loop gain can be adjusted using the resistance values R_{Cu} and R_{Cu3} in the non-inverting amplifier in the circuit for measuring the copper ion concentration.

3. Experimental Setup and Results

The miniaturized WQDS was implemented to measure the water quality parameters of temperature, pH value, electrical conductivity, and copper ion concentration. The temperature measurement uses an NTC thermistor in the temperature sensor, and its characteristic has good linearity owing to its voltage divider design. The measurement circuit for the electrical conductivity is composed of gold-plated bipolar electrodes, which can reduce the possibility of reaction with the measurement object and thus protect the sensing electrode to some extent. The improved pH-sensing electrode uses FTO conductive glass as a sensing film material, and the reference electrode is made of an unreactive material. Many sensing terminals are based on commercially available stable pen-type sensors. This study mainly achieved the same effect as commercially available sensors at a low cost. Here, the reference electrode providing a stable electrode potential is composed of an FTO conductive glass substrate. The dual gold-plated electrodes at the contact point have good electrical conductivity and noise reduction characteristics. The three-electrode method and SWV method are implemented on the electrodes used to measure the copper ion concentration. The three-electrode method is used to improve the sensitivity and linearity of the copper ion concentration measurement at trace concentrations while improving the accuracy and reducing the manufacturing cost, and the measurement

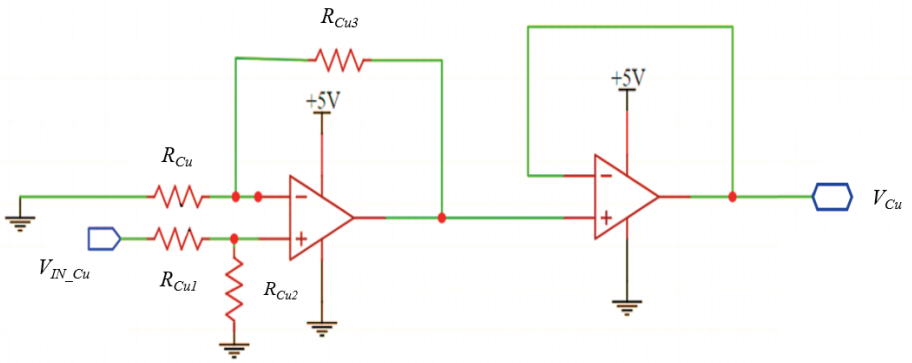

Fig. 5. (Color online) Circuit in the module for measuring the copper ion concentration.

concentration range is from 5×10^{-8} to 5×10^{-1} M. The improved pH-sensing electrode and the reference electrode are fabricated on the glass substrate in the form of three layers. The first layer of the material is FTO, the second layer is a platinum layer located outside the pH-sensing area, and the third layer is the gold-plated layer on the contact. The sensing electrodes of the water sensors in the miniaturized WQDS are shown in Fig. 6.

Standard solutions of different concentrations were used for testing in this study. The water quality characteristics of the standard solutions were evaluated using a precision instrument and then monitored by the miniaturized WQDS. The continuous monitoring time is 180 min and the measurement rate is five times per 18 min. Calibration curves are obtained from the physical quantities corresponding to the various measurements using the sensing electrodes, which are converted to voltage values by the MCU using relational expressions. To enable comparisons, calibration curves of the water quality parameters are obtained by the WQDS, then the curves are adjusted by performing measurements using a precision instrument. The better the linear regression line fits the measurement values in comparison with the average, the closer the coefficient of determination R^2 of the calibration curve is to 1. The average value is utilized to obtain the single-point error. The standard deviation, the single-point multi-time solution measurement scale, and the single-point multi-time solution measurement error are required and replaced with the extreme value of the multi-time measurement. The calibration measurement has n samples, marked $y_1, y_2, ..., y_n$, so the average value $\overline{y}$ is in the form of

$$\overline{y} = \frac{1}{n}\sum_{i=1}^{n} y_i \ . \tag{5}$$

The coefficient of determination R^2 is defined as

$$R^2 \equiv 1 - \frac{SS_R}{SS_T} = 1 - \frac{\sum (y_i - f_i)^2}{\sum (y_i - \overline{y})^2}, \tag{6}$$

where SS_T is the total sum of squares and SS_R is the sum of squares of residuals.

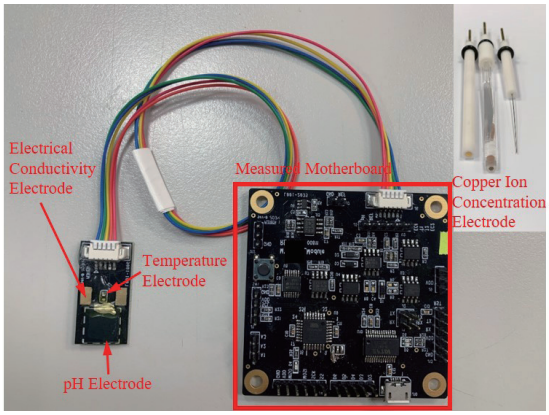

Fig. 6. (Color online) Sensing electrodes of the water sensors in the miniaturized WQDS.

3.1 Monitoring of temperature

The experimental verification of the temperature sensing electrode in the WQDS depends on the difference between the measurement temperature from the MCU on the measurement motherboard and the actual temperature. The temperature in the experiment was increased from 10 to 40 °C using a hot plate, and the temperature was monitored with a thermocouple simultaneously. The experimental setup for the temperature measurement is shown in Fig. 7.

The temperature sensing electrode of the WQDS shows a sensitivity of −24.745 °C/V in the temperature range from 10 to 40 °C, and has excellent linearity with a determination coefficient of $R_{Temp}^2 = 0.9995$. The temperature accuracy is computed as 0.02% in the measurement range. During the measurement with increasing temperature, the temperature sensing electrode was placed in deionized water (DI water). The voltage of the MCU on the measurement motherboard was recorded and converted using the value of sensitivity, and then the heating temperature of the water samples was monitored. An *X*–*Y* scatter plot of the measurement temperatures was drawn to obtain a calibration curve as shown in Fig. 8.

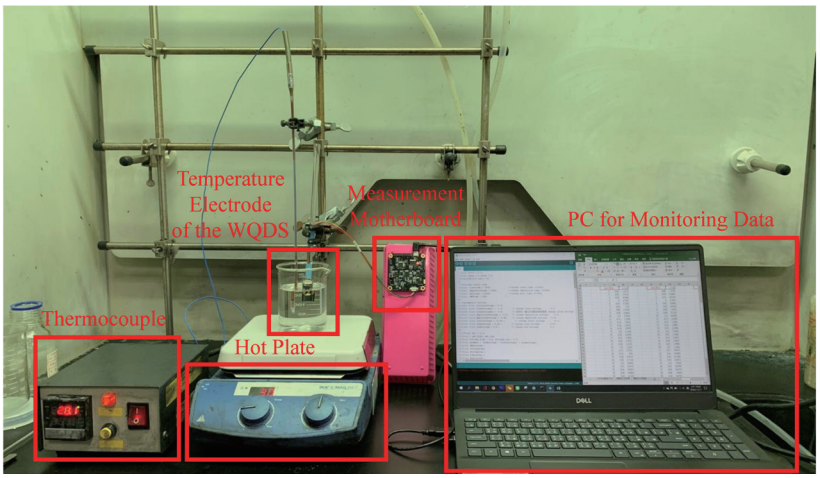

Fig. 7. (Color online) Experimental setup for temperature measurement.

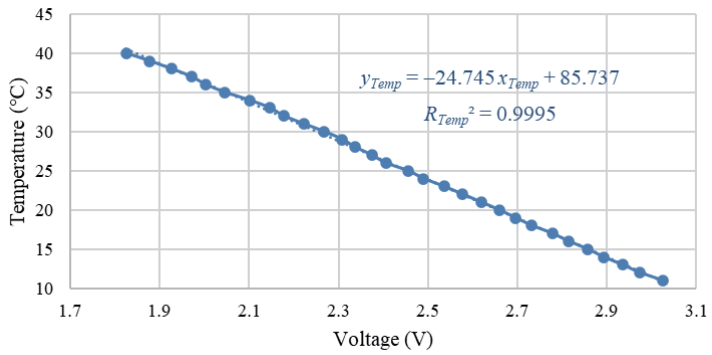

Fig. 8. (Color online) Calibration curve of the temperature sensing electrode in the WQDS.

3.2 Monitoring of pH value

An Arduino Leonardo was used as the main MCU in this study to detect the electric potential of the FTO film, and the ADC values were recorded then saved to a PC. The experimental setup for measuring pH values is shown in Fig. 9.

The pH calibration verification experiment was performed by comparing the voltage of the MCU on the motherboard and the actual pH values. The measurement range was from pH 4.0 to 10.0, and three different standard solutions with pH values of 4.0, 7.0, and 10.0 were chosen. The accuracy of the pH value is 0.01% in the measurement range. The improved pH-sensing electrode of the WQDS has a sensitivity of −3.74 pH/V and good linearity (determination coefficient R_{pH}^2 = 0.9985). The Arduino Leonardo was also utilized to acquire the voltage of the MCU on the motherboard, which is the electric potential difference of the FTO membrane. The calibration curve of the improved pH-sensing electrode in the WQDS is shown in Fig. 10.

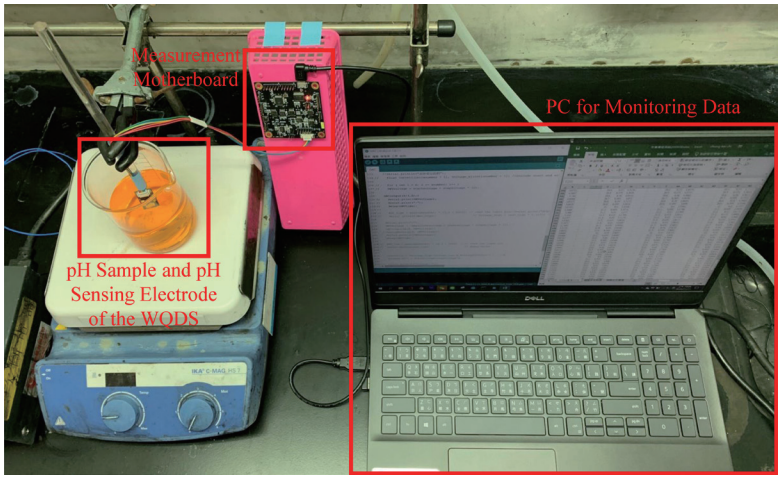

Fig. 9. (Color online) Experimental setup for measuring pH values.

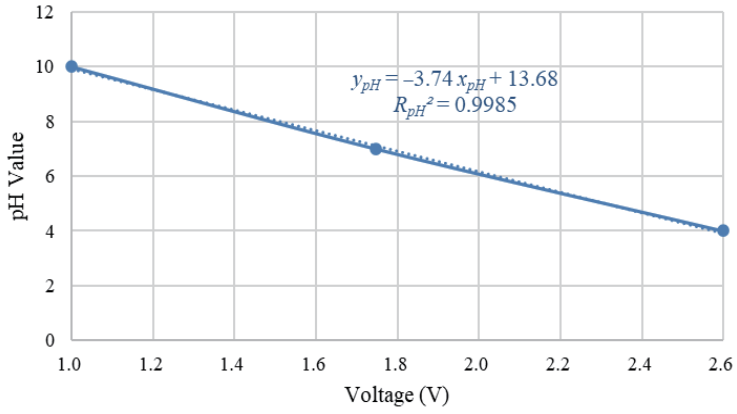

Fig. 10. (Color online) Calibration curve of the improved pH-sensing electrode in the WQDS.

3.3 Monitoring of electrical conductivity

The experimental setup for measuring electrical conductivity is shown in Fig. 11. A titration method was utilized to verify the electrical conductivity calibration. In this method, DI water was added to saturated brine (electrical conductivity = 5.07 mS/cm) until the voltage dropped to zero (electrical conductivity = 0.005 mS/cm). During the titration process, a portable electrical conductivity meter was used to measure the electrical conductivity, and the values of the electrical conductivity and the voltage of the MCU on the measurement motherboard were recorded at the same time.

The calibration curve of the electrical conductivity electrode in the WQDS is shown in Fig. 12. During the titration process, the saturated brine was added to the DI water until the voltage was raised to 4 V. Next, the titration using DI water was performed again until the voltage returned to 0 V. The highest and lowest limits of the saturation voltage were 4 and 0 V,

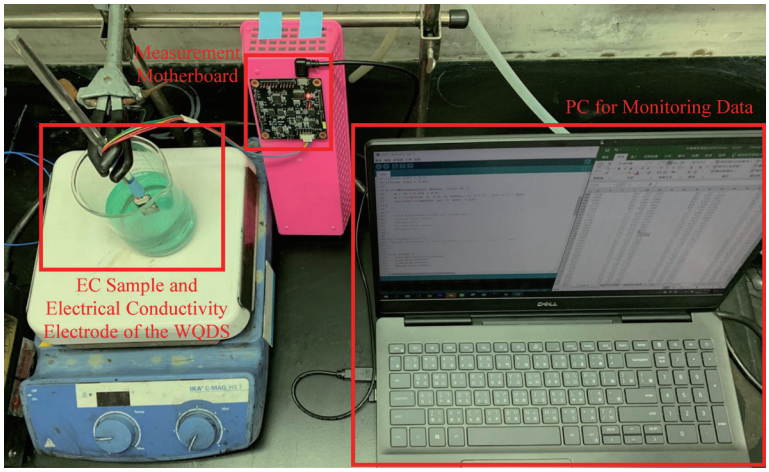

Fig. 11. (Color online) Experimental setup for measuring electrical conductivity.

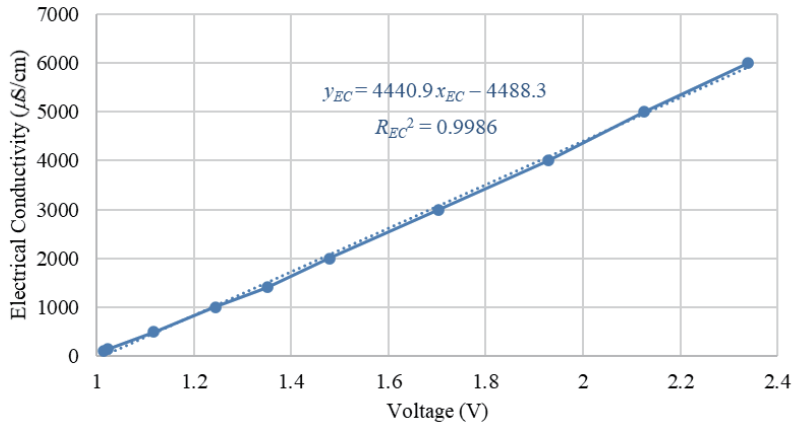

Fig. 12. (Color online) Calibration curve of the electrical conductivity electrode in the WQDS.

respectively. During the titration process, the voltage and electrical conductivity values were recorded at the same time. The electrical conductivity of the WQDS shows a sensitivity of 4.44 mS/V·cm in the measurement range from 0 to 6.0 mS/cm. The accuracy of the electrical conductivity is 1.7% in the measurement range and its linear determination coefficient of R_{EC}^2 = 0.9986 is high enough to measure the electrical conductivity in the WQDS.

3.4 Monitoring of copper ion concentration

Figure 13 shows the experimental setup used for square wave anodic stripping voltammetry to measure the copper ion concentration. The calibration curve of the copper ion concentration electrodes in the WQDS is shown in Fig. 14. The measurement range of the copper ion

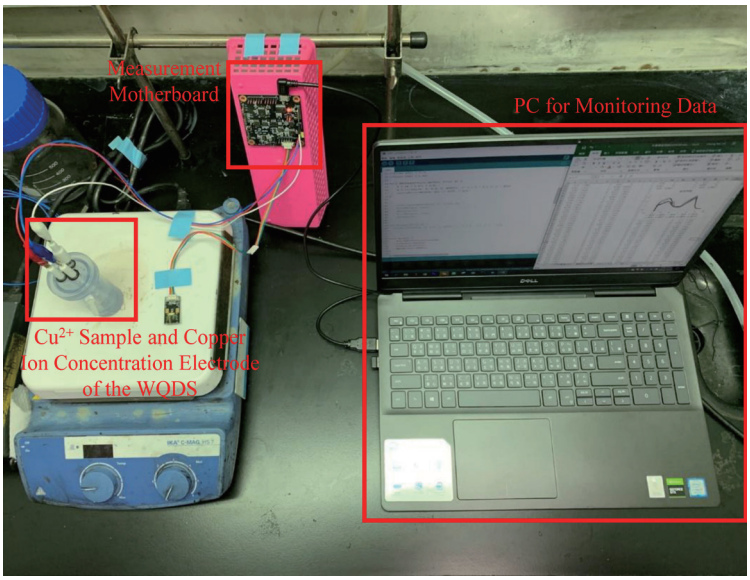

Fig. 13. (Color online) Experimental setup for measuring copper ion concentration.

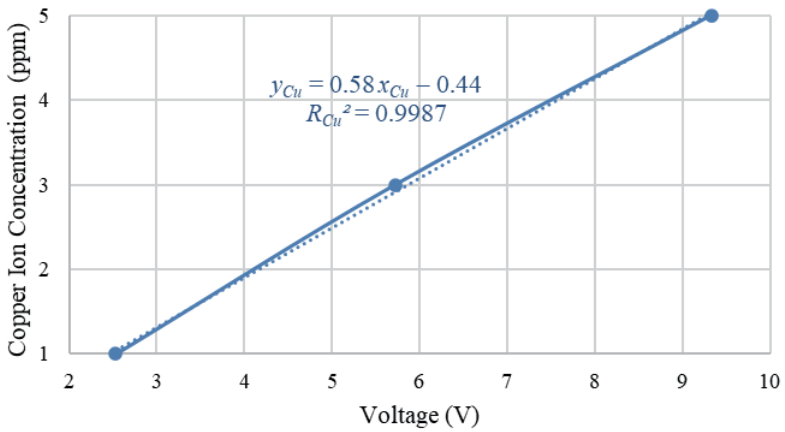

Fig. 14. (Color online) Calibration curve of copper ion concentration electrodes in the WQDS.

concentration was from 0 to 5.0 ppm, and the experimental values of the copper ion concentration were set as 5.0, 3.0, and 1.0 ppm. The sensitivity of the three electrodes used to measure the concentration of copper ions was found to be 0.58 ppm/V, and the sensing characteristic of the copper ion concentration electrodes has good linearity with a determination coefficient of R_{Cu}^2 = 0.9987. The accuracy of the copper ion concentration was calculated as 0.96% in the measurement range. During the measurement process, the three-electrode signal was transmitted to the copper ion measurement circuit. In addition, the monitoring data from the copper ion measurement circuit via the measurement motherboard was simultaneously recorded by the PC.

4. Conclusions

In this study, a multifunctional WQDS has been developed that can simultaneously detect four different water parameters: temperature, pH value, electrical conductivity, and copper ion concentration. In our water-monitoring experiments, the detection conditions were set up as a continuous monitoring period of 180 min and a measurement rate of five times per 18 min. The sensitivities of the temperature-sensing electrode, improved pH-sensing electrode, electrical conductivity electrodes, and copper ion concentration electrodes of the WQDS are −24.745 °C/V (range: 10–40 °C), −3.74 pH/V (range: pH 4.0–10.0), 4.44 mS/V·cm (range: 0–6.0 mS/cm), and 0.58 ppm/V (range: 0–5.0 ppm), respectively. The sensors have exceptionally high linearity and their coefficients of determination are R_{Temp2} = 0.9995, R_{pH}^2 = 0.9985, R_{EC}^2 = 0.9986, and R_{Cu}^2 = 0.9987, respectively. It was found by measurement and calculation that the accuracies of the temperature, pH value, electrical conductivity, and copper ion concentration of the WQDS are 0.02, 0.01, 1.7, and 0.96% in the measurement ranges, respectively. Therefore, the WQDS has good potential for use in the water-monitoring field and for the precision detection of various water quality parameters.

References

1 N. A. Cloete, R. Malekian, and L. Nair: IEEE Access **4** (2016) 3975. https://doi.org/10.1109/ACCESS.2016.2592958
2 H. C. Yu, M. Y. Tsai, Y. C. Tsai, J. J. You, C. L. Cheng, J. H. Wang, and S. J. Li: Sensors **19** (2019) 1. https://doi.org/10.3390/s19173758
3 F. Yuan, Y. Huang, X. Chen, and E. Cheng: IEEE Access **6** (2018) 61535. https://doi.org/10.1109/ACCESS.2018.2876336
4 X. Wang, Y. Wang, H. Leung, S. C. Mukhopadhyay, S. Chen, and Y. Cui: IEEE Access **7** (2019) 173157. https://doi.org/10.1109/ACCESS.2019.2956568
5 A. Shen, S. B. Kim, C. Bailey, A. W. K. Ma, and S. Dardona: IEEE Sens. J. **18** (2018) 9105. https://doi.org/10.1109/JSEN.2018.2869850
6 G. Zhao and G. Liu: IEEE Sens. J. **18** (2018) 5645. https://doi.org/10.1109/JSEN.2018.2845306
7 Y. W. Fen, W. M. M. Yunus, and N. A. Yusof: Sens. Mater. **23** (2011) 325. https://doi.org/10.18494/SAM.2011.723
8 J. van der Spiegel, I. Lauks, P. Chan, and D. Babic: Sens. Actuators, B **4** (1983) 291. https://doi.org/10.1016/0250-6874(83)85035-5
9 D. E. Yates, S. Levine, and T. W. Healy: J. Chem. Soc. Faraday Trans. I **70** (1974) 1807. https://doi.org/10.1039/F19747001807
10 R. B. Huang and Y. F. Zheng: Micro Nano Lett. **9** (2014) 766. https://doi.org/10.1049/mnl.2014.0224
11 R. Ravikumar, L. H. Chen, M. M. Xin Hui, and C. C. Chan: J. Light. Technol. **37** (2019) 2778. https://doi.org/10.1109/JLT.2018.2874171

12 Z. Wu, J. Wang, C. Bian, J. Tong, and S. Xia: Micromachines **11** (2020) 1. https://doi.org/10.3390/mi11010063
13 Y. Qin, A. U. Alam, S. Pan, M. M. R. Howlader, R. Ghosh, N. X. Hu, H. Jin, S. Dong, C. H. Chen, and M. J. Deen: Sens. Actuators, B **255** (2018) 781. https://doi.org/10.1016/j.snb.2017.07.188
14 B. Zhou, C. Bian, J Tong, and S Xia: Sensors **17** (2017) 1. https://doi.org/10.3390/s17010157.
15 H. Wan, Q. Sun, H. Li, F. Sun, N. Hu, and P. Wang: Sens. Actuators, B **209** (2015) 336. https://doi.org/10.1016/j.snb.2014.11.127
16 N. R. Moparthi, C. Mukesh, and P. V. Sagar: Proc. 2018 4th Int. Conf. Advances in Electrical Electronics, Information, Communication and Bio-Informatics (AEEICB) 109–113.
17 J. Lee, S. Kim, and H. Shin: Sensors **21** (2021) 1. https://doi.org/10.3390/s21041346
18 V. Mirceski, S. Skrzypek, and L. Stojanov: ChemTexts **4** (2018), 1. https://doi.org/10.1007/s40828-018-0073-0
19 L.-D. Chen, W.-J. Wang, and G.-J. Wang: Biosensors **11** (2021) 1. https://doi.org/10.3390/bios11040109
20 G. M. Ali, R. H. Dhaher, and A. A. Abdullateef: Proc. 2015 3rd Int. Conf. Technological Advances in Electrical, Electronics and Computer Engineering (TAEECE) 234–238.
21 T. Yuwono, W. B. Pramono, I. Ardi, L. Hakim, and M. Ismail: Proc. 2015 Int. Conf. Space Science and Communication (IconSpace) 84–88.

About the Authors

Hsing-Cheng Yu received his M.S. and Ph.D. degrees from the Department of Mechanical Engineering, National Chiao Tung University, Taiwan, in 2002 and 2010, respectively. From 2002 to 2011, he was a researcher at the Industrial Technology Research Institute, Taiwan. He is currently an associate professor in the Department of Systems Engineering and Naval Architecture, National Taiwan Ocean University, Taiwan. His research interests include measurement engineering and sensing technology, optomechatronics system integration, actuator design and motor drive control, and ocean energy systems. (hcyu@ntou.edu.tw)

Chung-Kai Chi received his B.S. degree from the Department of Mechanical Engineering, Chinese Culture University, Taiwan, in 2019. He is currently in the master's program of the Department of Systems Engineering and Naval Architecture, National Taiwan Ocean University, Taiwan. His research interests are in the fields of sensor technology and system integration. (10851025@mail.ntou.edu.tw)

Ming-Yang Tsai received his B.S. degree from National Taiwan Ocean University, Taiwan, in 2015. He is currently in the master's program of the Department of Systems Engineering and Naval Architecture, National Taiwan Ocean University, Taiwan. His research interests are in the fields of sensor technology and system integration. (10751015@ntou.edu.tw)

Chun-Lin Cheng received his B.S. and M.S. degrees from the Departments of Mechanical and Mechatronic Engineering and Systems Engineering and Naval Architecture, National Taiwan Ocean University, Taiwan, in 2015 and 2017, respectively. From 2017 to 2020, he was a researcher at the Industrial Technology Research Institute, Taiwan. He is currently an engineer in Advantest Corporation. His research interests are in the fields of signal processing, sensor technology, and system integration.
(10451032@email.ntou.edu.tw)

Jung-How Wang received his M.S. and Ph.D. degrees from the Department of Engineering Science, National Cheng Kung University, Taiwan, in 2004 and 2008, respectively. He is currently a researcher at the Industrial Technology Research Institute, Taiwan. His research interests lie in microfluidics systems and sensors and their applications to wearable devices and water quality monitoring. (junghow@itri.org.tw)

Szu-Ju Li received his M.S. and Ph.D. degrees from the Department of Electrical Engineering, National Central University, Taiwan, in 2002 and 2007, respectively. He is currently a researcher at the Industrial Technology Research Institute, Taiwan. His research interests focus on the simulation and modeling of semiconductor devices, AIoT sensor devices, system integration, wearable electronics circuits, and device interactions. (SJ_Li@itri.org.tw)